# Transfer of micro and nano-photonic silicon nanomembrane waveguide devices on flexible substrates

**Afshin Ghaffari [1], Amir Hosseini [1], Xiaochuan Xu[1], David Kwong[1], Harish Subbaraman[2], and Ray T. Chen[1]**

[1]*Microelectronics Research Center, The University of Texas at Austin, Austin, TX 78758, USA*
[2]*Omega Optics, Inc., 10306 Sausalito Dr, Austin, TX, 78759, USA*
*raychen@uts.cc.utexas.edu*

**Abstract:** This paper demonstrates transfer of optical devices without extra un-patterned silicon onto low-cost, flexible plastic substrates using single-crystal silicon nanomembranes. Employing this transfer technique, stacking two layers of silicon nanomembranes with photonic crystal waveguide in the first layer and multi mode interference couplers in the second layer is shown, respectively. This technique is promising to realize high density integration of multilayer hybrid structures on flexible substrates.



**OCIS codes:** (220.4000) Microstructure fabrication; (220.4241) Nanostructure fabrication; (040.6040) Silicon.

## References and links

1. F. Cavallo, and M. G. Lagally, "Semiconductors turn soft: inorganic nanomembranes," Soft Matter **6**(3), 439–455 (2010).
2. G. Qin, H. C. Yuan, G. K. Celler, W. Zhou, and Z. Ma, "Flexible microwave PIN diodes and switches employing transferrable single-crystal Si nanomembranes on plastic substrates," J. Phys. D Appl. Phys. **42**(23), 234006 (2009).
3. D.-H. Kim, J. A. Rogers; " Stretchable electronic*s:* Materials strategie*s and* devices," Adv. Mater. **20**(24), 4887–4892 (2008).
4. M. G. Legally, "Group IV Crystalline Nanomembranes: Materials, Technology, and Potential Applications," Proc. IEEE 4244–4403, 104–106 (2009).
5. E. Menard, R. G. Nuzzo, and J. A. Rogers, "Bendable single crystal silicon thin film transistors formed by printing on plastic substrates," Appl. Phys. Lett. **86**(9), 093507 (2005).
6. F. Niklaus, E. Kalvesten, and G. Stemme, "Wafer-level membrane transfer bonding of polycrystalline silicon bolometers for use in infrared focal plane arrays," J. Micromech. Microeng. **11**(5), 509–513 (2001).
7. M. J. Zablocki, A. S. Sharkawy, O. Ebil, D. W. Prather, "Nanomembrane enabled nanophotonic devices," Proc. SPIE **7606**, 76060V (2010).
8. W. Zhou, Z. Ma, H. Yang, Z. Qiang, G. Qin, H. Pang, L. Chen, W. Yang, S. Chuwongin, and D. Zhao, "Flexible photonic-crystal Fano filters based on transferred semiconductor nanomembranes," J. Phys. D Appl. Phys. **42**(23), 234007 (2009).
9. H. C. Yuan, Z. Ma, M. M. Roberts, D. E. Savage, and M. G. Lagally, "High-speed strained-single-crystal-silicon thin-film transistors on flexible polymers," J. Appl. Phys. **100**(1), 013708 (2006).
10. H. C. Yuan, G. K. Celler, and Z. Ma, "7.8-GHz flexible thin-film transistors on a low-temperature plastic substrate," J. Appl. Phys. **102**(3), 034501 (2007).
11. H.-C. Yuan, J. Shin, G. Qin, L. Sun, P. Bhattacharya, M. G. Lagally, G. K. Celler, and Z. Ma, "Flexible photodetectors on plastic substrates by use of printing transferred single-crystal germanium membranes," Appl. Phys. Lett. **94**(1), 013102 (2009).
12. F. V. Laere, G. Roelkens, M. Ayre, J. Schrauwen, D. Taillaert, D. V. Thourhout, T. F. Krauss, and R. Baets, "Compact and Highly Efficient Grating Couplers Between Optical Fiber and Nanophotonic Waveguides," J. Lightwave Technol. **25**(1), 151–156 (2007).
13. T. K. Saha, and W. Zhou, "High efficiency diffractive grating coupler based on transferred silicon nanomembrane overlay on photonic waveguide," J. Phys. D Appl. Phys. **42**(8), 085115 (2009).
14. R. Ulrich, and T. Kamiya, "Resolution of self-images in planar optical waveguides," J. Opt. Soc. Am. **68**(5), 583–592 (1978).

#129442 - $15.00 USD Received 2 Jun 2010; revised 12 Aug 2010; accepted 16 Aug 2010; published 3 Sep 2010

15. J. Z. Huang, R. Scarmozzino, and R. M. Osgood, Jr., "A new design approach to large input/output number multimode interference couplers and its application to low-crosstalk WDM routers," IEEE Photon. Technol. Lett. **10**(9), 1292–1294 (1998).
16. A. Hosseini, D. N. Kwong, C.-Y. Lin, B. S. Lee, and R. T. Chen, "Output Formulation for Symmetrically-Excited one-to-N Multimode Interference Coupler," IEEE J. Sel. Top. Quant, Elect. **6**(1), 53–60 (2010).
17. S. F. Mingaleev, A. E. Miroshnichenko, Y. S. Kivshar, and K. Busch, "All-optical switching, bistability, and slow-light transmission in photonic crystal waveguide-resonator structures," Phys. Rev. E Stat. Nonlin. Soft Matter Phys. **74**(4), 046603 (2006).
18. T. Baba, "Slow light in photonic crystals," Nat. Photonics **2**(8), 465–473 (2008).
19. P. Sanchis, P. Bienstman, B. Luyssaert, R. Baets, and J. Marti, "Analysis of butt coupling in photonic Crystals," IEEE J. Quantum Electron. **40**(5), 541–550 (2004).
20. P. Pottier, M. Gnan, and R. M. De La Rue, "Efficient coupling into slow-light photonic crystal channel guides using photonic crystal tapers," Opt. Express **15**(11), 6569–6575 (2007).
21. G. M. Cohen, P. M. Mooney, V. K. Paruchuri, and H. J. Hovel, "Dislocation-free strained silicon-on-silicon by in-place bonding," Appl. Phys. Lett. **86**(25), 251902 (2005).

## 1. Introduction

The applications of flexible electronic and photonic structures have significant engineering importance [1]. So far, most of the flexible electronics research has been based on organic, polymer and amorphous semiconductor. Single crystal nanomembranes are considered as practical alternatives for organic semiconductors. By using nanomembranes, single-crystal materials with different crystal orientations or different compositions can be integrated for applications requiring stacking of hybrid layers that cannot be obtained by planar growth techniques. Also, stackability permits access to three dimensional structures and devices with novel optoelectronic, photonic, or electronic properties [1].

In the case of silicon nanomembranes, it has been shown that a single crystal layers can be obtained by etching the buried oxide in silicon on insulator (SOI). The resulting silicon nanomembranes are then transferred onto flexible substrates [1]. Over the past few years, several groups have investigated similar techniques for silicon nanomembrane transfer and stacking [1–8]. High performance flexible electronics, such as photodetectors, based on transferable silicon nanomembranes were reported [9–11]. Qin *et al* reported fabrication of flexible RF/microwave PIN diodes on flexible substrate using a direct flip transfer technique [2]. Zhou *et al* demonstrated Fano filters on transferred silicon nanomembranes on flexible substrates using a wet transfer process [8]. Recently, Zablocki *et al* reported a successful transfer of one layer of optical switch node including eight photonic crystal waveguides patterned on SOI onto a flexible substrate, and also stacking of two layers of patterned silicon nanomembrane onto a glass substrate [7]. However, all the unattached and un-patterned silicon around the device is also transferred together with the device.

One important challenge to utilize optical devices on flexible substrates is the input signal coupling. This especially seems challenging in the case of multilayer structures, since techniques such as butt-coupling or end-fire coupling (e.g. using lensed fiber) require defect-free facets. One possible technique is to use grating coupling [12,13], which has been already used to excite silicon nanomembrane waveguides transferred on another SOI substrate [13]. Transparency allows devices such as photo-detectors and photocells to operate in the buried layers of a multilayer structure. Additionally, transparent structure allows easier multilayer alignments. To the best of our knowledge, transfer of small (~10s of micrometers) photonic devices without transferring the large unpatterned and unattached silicon nonomembranes has not been reported before. In this paper, we present a modified transfer technique that enables transfer of micro and nanophotonic silicon devices without the un-patterned and unattached silicon nanomembrane. We use a pattern inversion technique to fabricate structures, such as multimode interference patterns without unattached silicon nanomembranes. In case of devices, such as photonic crystal waveguides, an extra lithography step is used to remove the un-patterned silicon nanomembranes surrounding the device. Using this modified transfer and planarization technique, we present single and double layer nanomembrane transfer onto a

#129442 - $15.00 USD Received 2 Jun 2010; revised 12 Aug 2010; accepted 16 Aug 2010; published 3 Sep 2010

flexible substrate. This technique can be used to realize multilayer flexible photonic structures containing optical devices on different layers on flexible substrates.

We first present a design for multimode interference couplers and highly dispersive photonic crystal waveguides in Section 2. Fabrication and transfer techniques are presented in Section 3 and 4, respectively.

## 2. Design

### *2.1 Multimode interference couplers*

Multimode interference (MMI) devices based on self-imaging are key components in photonic integrated circuits (PICs). 1xN MMI-based beam splitters have been theoretically and experimentally investigated [14–16]. Figure 1 shows a schematic of a 1xN MMI splitter. The multimode waveguide section consists of a $W_{MMI}$ wide and $L_{MMI}$ long core. In the case of a symmetric excitation, such as a 1xN coupler excited by the fundamental mode of the input waveguide, the required length for N-fold self imaging is given as

$$L_{MMI} = \frac{3rL_{\pi}}{4N}, \tag{1}$$

where $L_{\pi}=4n_{eff}W_e^2/3\lambda_0$. $\lambda_0$ is the free-space wavelength, $r$ is an integer number, $W_e$ is the effective width including the penetration depth due to the Goose-Hahnchen shift [16]. $n_{eff}$ is the effective index of the fundamental mode of an infinite slab waveguide with same thickness and claddings. We have designed 1x4 ($W_{MMI}$=20.0μm, $L_{MMI}$=184.2μm) and 1x12 ($W_{MMI}$=60.0μm, $L_{MMI}$=553.4μm) MMIs for silicon nanomembrane thickness $h$=230nm. For the output near field testing, the output waveguides are fanned out to have 30μm channel-to-channel spacing.

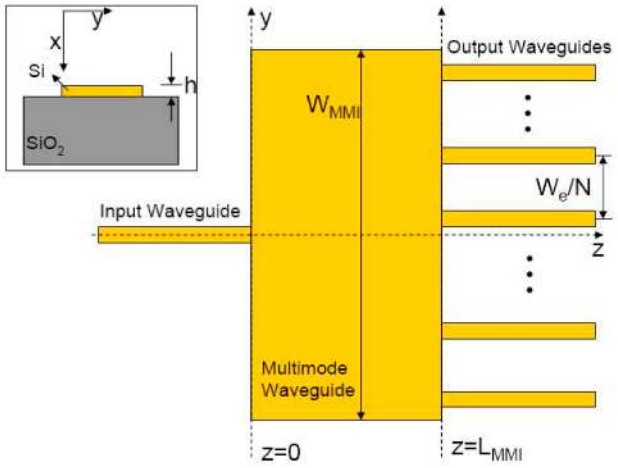


Fig. 1. A schematic of a 1xN MMI beam splitter. Inset is a cross section schematic of the SOI waveguiding structure.

### *2.2 Highly dispersive photonic crystal waveguides*

Despite being narrow bandwidth, highly dispersive photonic crystal waveguides provide tunable delay lines by simply tuning the input light wavelength within less than 10nm bandwidth. The operating principles are similar to those of the highly dispersive photonic crystal fibers [17]. The group velocity of a guided mode is calculated as the derivative of the angular frequency over the wavevector.

#129442 - $15.00 USD Received 2 Jun 2010; revised 12 Aug 2010; accepted 16 Aug 2010; published 3 Sep 2010

$$v_g \equiv \frac{\partial \omega}{\partial k} \tag{2}$$

Group index is $n_g=c/v_g$, where $c$ is the speed of light. The derivative of the reciprocal group velocity over the frequency gives the group velocity dispersion, *GVD*, as follows

$$GVD = \frac{\partial\left(1/v_g\right)}{\partial \omega} \tag{3}$$

Thus, if the input light wavelength is changed from $\lambda_0$ to $\lambda_1$, the change in the traveling time is given as

$$\Delta t = L\int_{\lambda_0}^{\lambda_1} GVD(\lambda)\cdot d\lambda, \tag{4}$$

where, $L$ is the length of PCW. Based on (4), high *GVD* values are needed for large delay time, which means that the PC band ($\omega$ versus $k$) should be away from being flat. At the same time, we note that delay time depends on the *GVD* values not the $n_g$, and since propagation loss increases with $n_g$, it is important to engineer the photonic band to have largest *GVD* values at the lowest possible $n_g$ values. Experimental studies have shown that for group indices larger than about 30, the propagation loss can be excessively high [18].

A PCW structure with input and output waveguide is shown in Fig. 2(a). A PCW is usually realized by removing one row of air holes. In our case, the photonic crystal is a hexagonal lattice, air holes (red) in silicon slab (gray). In order to engineer the band structure of the PCW, we tune 4 parameters. We tune the size of the gap ($g$) between the two innermost rows, which without any change is $a\sqrt{3}$, where $a$ is the lattice constant. For a tuned structure, $g$ is given as $(1+dW)a\sqrt{3}$. We also tune the radii of the hole in the inner rows ($r_1$), the second inner row ($r_2$) and all other rows ($r$) as shown in Fig. 2. Input/output tapers are used to reduce the insertion loss [19,20]. Note that the structure holds its inversion symmetry with respect to the PCW gap. By changing $dW$, $r_1$, $r_2$ and $r$, we optimize the band structure for highly dispersive applications by minimizing the total propagation loss. We use BandSolve™ to simulate the PCWs. The band structure for $r$=0.262$a$, $r_1$=0.338$a$, $r_2$=0.202$a$, and $dW$=0 is shown in Fig. 2(b).

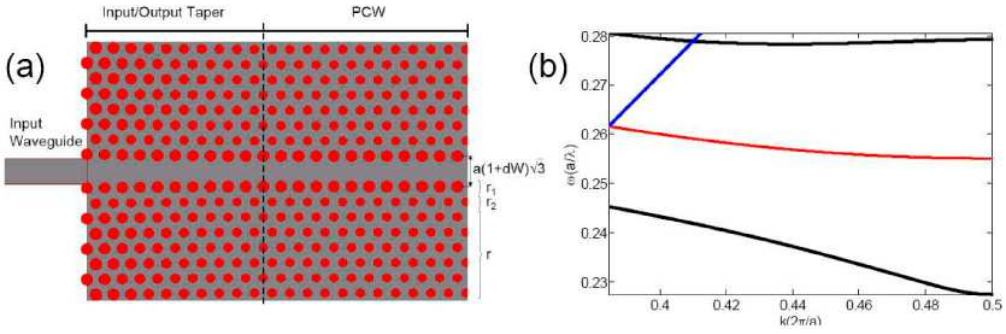


Fig. 2. (a) A schematic of the band-engineered PCW structure and the input/output coupling taper structure. The design parameters ($r_1$, $r_2$, $r_3$ and $dW$) are shown. The input and output tapered PCW couplers are mirror images of each other in the actual implementation. (b) Band structure of the optimized photonic crystal waveguide (red). The blue and black lines show the light line (n=1.45) and the band gap edges, respectively.

#129442 - $15.00 USD Received 2 Jun 2010; revised 12 Aug 2010; accepted 16 Aug 2010; published 3 Sep 2010

## 3. Fabrication and characterization of Si-nanomembrane devices

### *3.1 1x4 and 1x12 multimode interference couplers*

We fabricated multimode interference coupler for transfer purpose using pattern inversion technique. The advantage of this method is to readily have the device without any extra silicon. Figure 3(a) illustrates the pattern inversion steps used to fabricate multimode interference coupler on top of SOI. After electron beam lithography and developing, a 20 nm titanium layer is deposited and a standard lift-off process is used to remove the extra titanium. The pattern is transferred to the silicon oxide hard mask by reactive ion etching (RIE). The metallic layer is removed by piranha so that it does not cause absorption losses during optical testing. An HBr/Cl2 RIE etch is then used to transfer the pattern to the silicon layer. Figure 4(a) shows an SEM picture of the fabricated 1x12 multimode inference coupler.

### *3.2 Highly dispersive photonic crystal waveguides*

Photonic crystal waveguide devices are fabricated on commercially available SOI from SOITEC with 250nm top silicon layer. Figure 3(b) demonstrates the PCW fabrication steps. The silicon is first oxidized to create a 45nm thick top oxide layer which serves as a hard mask for the silicon etch. This oxidation consumes 20nm of silicon, leaving a final silicon thickness of 230nm. The photonic devices are patterned using a JEOL JBX600 electron beam lithography system. After developing, the resist pattern is transferred to the oxide mask using reactive ion etching (RIE). A HBr/Cl2 RIE etch is then used to transfer the pattern to the top silicon layer using the oxide as an etch mask. Piranha cleaning completes the process by removing the resist. Figure 4(b) shows the scanning electron microscopy (SEM) image of PCW including trenches. Having these large trenches reduces mask alignment tolerance required in later steps to remove extra silicon around device.

Figure 3(b) demonstrates our extra lithography steps to remove the un-patterned silicon around the device. Photoresist layer is spin coated on top of the device and patterned. The exposed photoresist is then developed and used as a mask to protect it during etching un-patterned silicon.

#129442 - $15.00 USD Received 2 Jun 2010; revised 12 Aug 2010; accepted 16 Aug 2010; published 3 Sep 2010

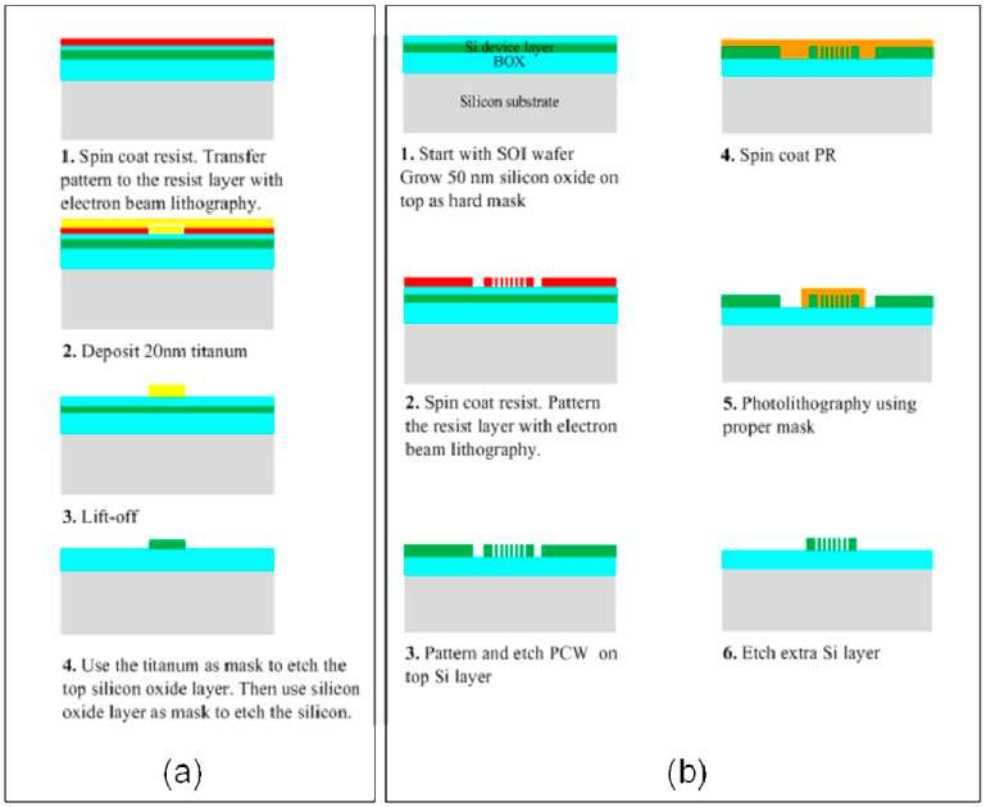


Fig. 3. (a) Fabrication process flow for multimode interference coupler, which includes pattern inversion through a lift-off process. (b) Fabrication process flow for photonic crystal waveguide, which includes removal of the un-patterned silicon nanomembrane.

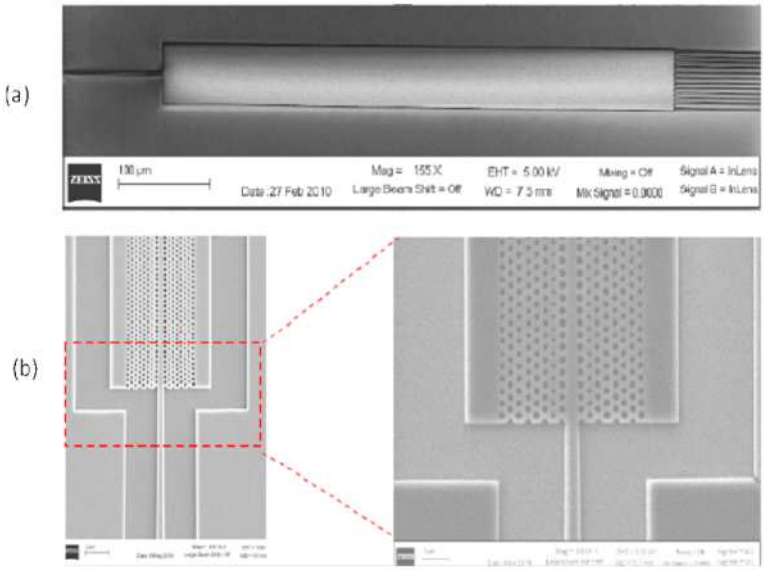


Fig. 4. SEM pictures of (a) 1x12 multimode interference coupler. (b) highly dispersive photonic crystal waveguide (before removal of un-patterned silicon nanomembrane).

#129442 - $15.00 USD Received 2 Jun 2010; revised 12 Aug 2010; accepted 16 Aug 2010; published 3 Sep 2010

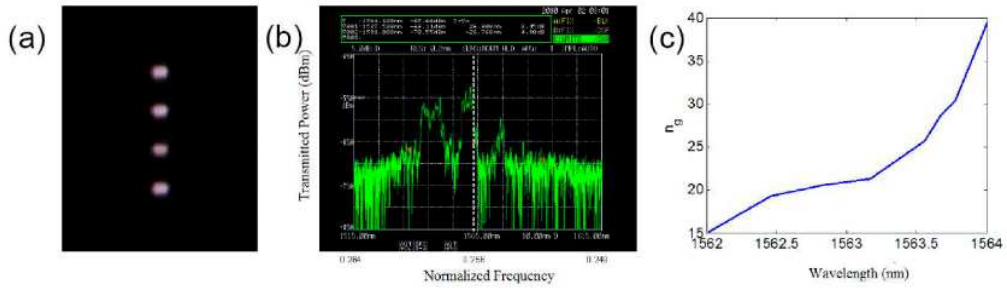


Fig. 5. (a) Output spots from 1x4 Multimode Interference coupler observed using an IR-CCD camera, (b) measured transmission spectrum of the fabricated photonic crystal waveguide (the dashed line indicates the band-edge), (c) measured group index ($n_g$) of the photonic crystal waveguide

After the fabrication, the devices are tested on a Newport six-axis autoaligner system. A filter combined with a polarizer was used to provide TE polarization for the input waveguides in the two devices. A polarization analyzer was also used to confirm the polarization state in the whole system. For the MMI, the output spots are top-down imaged using an IR-CCD camera. Figure 5(a) shows the top down near field image for the 1x4 MMI. From the output fiber scanning, the output uniformity was found to be 0.5dB and 0.7dB for the 1x4 and 1x12 MMIs, respectively. Uniformity is calculated as $10\log(P_{max}/P_{min})$, where $P_{max}$ and $P_{min}$ are the maximum and minimum power of the MMI output channels, respectively.

For the PCW, the transmission spectrum is measured on an optical spectrum analyzer and the group index is extracted from the spectral maxima and minima. These results are shown in Figs. 5(b) and (c), respectively. Based on Eqs. (2) and (3), a time delay of 35.3ps/mm is obtained for the PCW when the input wavelength is tuned from 1562.0nm to 1563.7nm, while the group index does not exceed 30. Note that the two transmission bands in Fig. 5(b) correspond to the two even PCW modes. The larger wavelength band is the PCW defect mode below the substrate line.

Surface-normal optical characterization of transferred photonic devices has been presented before, e. g. in the case of photonic-crystal Fano resonance based surface-normal optical filters in [8]. However, in-plane characterization of transferred optical devices is in itself extremely challenging due to the nature of the substrate and lack of a standard cleaving technique on such substrates. To the best of our knowledge, currently, there are no reports of optical characterization for in-plane optical devices. We have worked on developing a technique for cleaving devices on flexible hosts and generate perfect surfaces for end-fire optical coupling; the results will be reported elsewhere.

## 4. Transferring silicon nanomembrane onto flexible Kapton polyimide substrate

### *4.1 Single layer transfer*

Silicon nanomembrane transfer process can be done using either wet transfer or dry transfer techniques [1]. In wet transfer, the oxide layer is removed and the silicon nanomembrane is float-transferred onto a new substrate. Dry transfer can take place with either direct flip transfer [2] or stamp assisted transfer [5]. In the former method, an adhesion promoting layer is spun on the flexible substrate. Then, the target silicon nanomembrane is picked up directly by the flexible substrate from the original substrate. In stamp assisted process, a polydimethlsiloxane (PDMS) stamp is used to lift up the silicon nanomembrane. The stamp is pressed onto the new host substrate and slowly peeled off with shear force.

Unlike transferring photonic devices together with the un-patterned silicon nanomembrane, transferring individual photonic devices is much more difficult because photonic devices usually have large length to width ratio, with a smaller Van der Waals force compared to large area silicon nanomembrane. Furthermore, photonic devices are sensitive to

#129442 - $15.00 USD Received 2 Jun 2010; revised 12 Aug 2010; accepted 16 Aug 2010; published 3 Sep 2010

displacements, folding and breaks in the optical components. To solve these problems, we developed the transfer method as shown in Fig. 6(a). To prevent the shifting and breaking during the transfer process, an SU-8 (Micro-Chem) layer is introduced as a supporting layer. First, Hexamethyldisilazane (HMDS) is coated to promote the adhesion. Then SU-8 is spin-coated by 3000 rpm followed by a two-step pre-bake. Several windows are opened by photolithography to let the buffered hydrofluoric (BHF) solution reach the sacrificial layer. After post-bake and develop, hard-bake is utilized to further cross link the material. After leaving the prepared sample in 6:1 BHF for proper time, the sacrificial layer is removed and the SU-8 layer with photonic device settles down and bonds with the silicon substrate via Van der Waals forces [21]. Before spin coating the SU-8, the film needs to be cleaned with isopropyl alcohol (IPA) and deionized water. Finally, the substrate with the silicon nanomembrane is brought in contact face-down with the Kapton substrate and a slight pressure is exerted. The Kapton substrate is then peeled away carefully. The silicon nanomembrane is lifted off from the silicon substrate and transferred onto the Kapton substrate. With the supporting layer, micro photonic (MMI) and nanophotonic (PCW) devices with large length to width ratio are transferred successfully, as shown in Figs. 7(a) and (b).

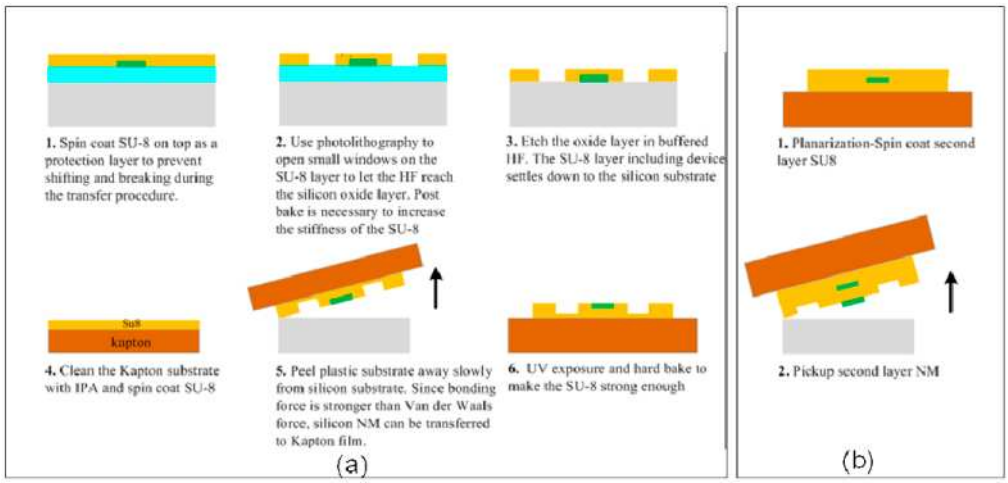


Fig. 6. (a) Silicon nanomembrane transfer process flow to transfer a single layer of nanomembrane onto a Kapton substrate, (b) additional steps required to perform transfer of a second layer on top of the first layer.

#129442 - $15.00 USD Received 2 Jun 2010; revised 12 Aug 2010; accepted 16 Aug 2010; published 3 Sep 2010

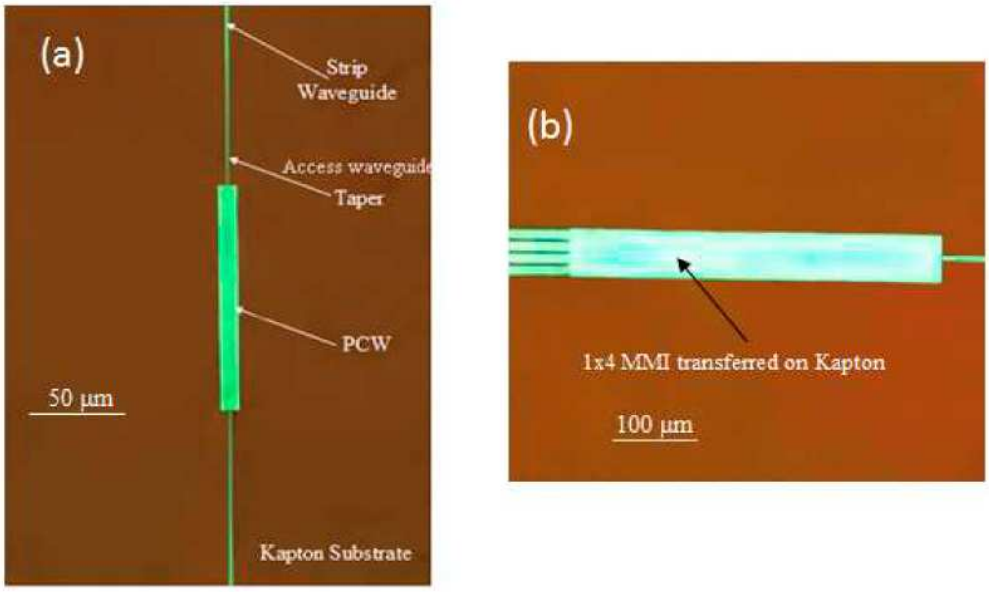


Fig. 7. Optical microscope images showing single layer transfer of (a) photonic crystal waveguide (PCW), and (b) 1x4 multimode interference coupler (MMI) on Kapton substrate

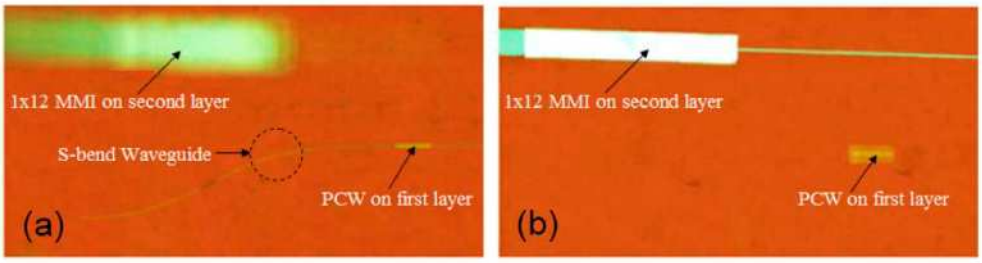


Fig. 8. Optical microscope image showing multilayer transfer of nanomembrane photonic devices on Kapton substrate. Two layer transfer of a photonic crystal waveguide (PCW) in the first layer and a 1x12 multimode interference coupler (MMI) on the second layer are shown. (a) shows the PCW (bottom layer) in focus, while (b) shows the 1x12 MMI coupler (top layer) in focus. The blurring of the devices in the other layers is due to the presence of a thick layer of SU-8 separating the two layers.

### *4.2. Multilayer transfer*

Silicon nanomembrane overlay and stacking photonic crystal waveguide onto plastic host substrate to integrate with other optical elements can be of great interest. Stacking nanomembranes layers sequentially can be realized by repeating previous transfer steps. After transferring the first nanomembrane layer, UV exposure following a post exposure bake is performed to cross-link the layer of SU-8, which makes it mechanically robust and highly stable as the host for second layer. Spinning another layer of SU-8 on top of the first layer provides a planarized surface for the second layer transfer as illustrated in Fig. 6(b). On this second layer of SU-8, the second nanomembrane is transferred. Figures 8(a) and (b) show the optical-microscope images of multimode interference coupler stacked on top of the first layer, which has a photonic crystal waveguide with an S-bend waveguide. In Fig. 8(a), the microscope is adjusted so that the PCW in the first layer in focus, and since the MMI in the second layer second layer separated by a thick SU-8 layer, it appears out of focus. Similarly,

#129442 - $15.00 USD Received 2 Jun 2010; revised 12 Aug 2010; accepted 16 Aug 2010; published 3 Sep 2010

in Fig. 8(b), the microscope is adjusted so that the MMI device in the second layer in focus, thus showing the PCW in the first layer out of focus.

## 5. Conclusion

We demonstrate transfer of single crystal silicon nanomembrane with optical devices onto flexible substrates. The photonic structures such as slow-light photonic crystal waveguides and multimode interference couplers released from SOI substrates are transferred onto low-cost flexible Kapton substrate. Using the silicon nanomembrane overlay transfer and stacking techniques, one can achieve a multilayer transfer leading to hybrid photonic integrated systems on low-cost flexible substrates.

## Acknowledgment

This research was funded by Air Force Office of Scientific Research (Dr. Gernot Pomrenke, Program Manager) under Contract number: FA9550-09-C-0212. [1] In this paper, design and simulations are done by A. Hosseini, device fabrication by X. Xu and D. Kwong, transferring device by A. Ghaffari and device characterization is done by A. Hosseini and H. Subbaraman.

#129442 - $15.00 USD Received 2 Jun 2010; revised 12 Aug 2010; accepted 16 Aug 2010; published 3 Sep 2010